

1 **Paleoceanographic implications of submarine scours and contourites around ancient**
2 **volcanoes, eastern Great Australian Bight**

3
4 Christopher A-L. Jackson*

5 Craig Magee

6 Esther R. Hunt-Stewart

7
8 *Basins Research Group (BRG), Department of Earth Science & Engineering, Imperial*
9 *College, Prince Consort Road, LONDON, SW7 2BP, UK*

10
11 **corresponding author email: c.jackson@imperial.ac.uk*

12
13 **ABSTRACT**

14
15 Thermohaline oceanic currents control local and global variations in climate, vegetation, and
16 biodiversity. Paleoceanographic studies typically use biostratigraphic and geochemical proxies
17 to reconstruct the dynamics of these currents in Earth's ancient oceans. Here we use 2D seismic
18 reflection data to interrogate the Middle Eocene-to-Recent stratigraphic record of ocean current
19 evolution within the Ceduna Sub-basin, which is located in the eastern Great Australian Bight.
20 These data show that 10–90 m deep, up to 3 km wide erosional scours, and <50 m thick,
21 sediment wave-like bedforms, probably generated by contour currents, are developed
22 throughout this carbonate-dominated succession. The scours are particularly well-developed at
23 one specific stratigraphic level, and define 'moats' encircling Middle Eocene shield volcanoes,
24 which, at that time, formed bathymetric highs. We suggest that sediment erosion, transport,
25 and deposition may record Middle Eocene initiation of the Leeuwin Current, one of the most
26 important ocean currents in the southern hemisphere. Deepest seabed scouring may reflect
27 middle Miocene waxing of the so-called 'proto-Leeuwin Current', possibly driven by changes
28 in ocean circulation patterns caused by the Miocene Global Optimum. The results of this
29 seismic reflection-based study are consistent with results derived from other
30 paleoceanographic proxies, thereby highlighting the key role seismic reflection data have in
31 understanding the occurrence, geographical distribution, and significance of ancient ocean
32 currents.

33
34 *end of abstract*

35

36 By influencing seawater temperature and salinity, ocean current activity controls regional and
37 global trends in climate and biodiversity. Determining past changes in thermohaline circulation
38 patterns in the world's oceans is thus important to understanding how climate and biodiversity
39 varied in deep time and, therefore, may change in the future (cf. "geological analogues" of
40 IPCC, 2007; see also e.g., Henderson, 2002; Wunsch, 2002; Rahmstorf, 2003; Wyrwoll et al.,
41 2009). Paleoceanographic analysis commonly relies on biostratigraphic and geochemical
42 proxy data, which: (i) are expensive to collect, and typically only collected on academic
43 scientific cruises (e.g. IODP); (ii) are spatially limited (i.e. collected over a relatively small
44 area within a discrete stratigraphic intervals); and (iii) do not typically provide a physical (i.e.
45 stratigraphic) record of the initiation, extent, and decay of oceanographic currents (e.g. von
46 Blackenburg, 1999; Henderson, 2002).

47 Seismic reflection data, which can provide relatively high-resolution images of the
48 Earth's subsurface (e.g. Cartwright and Huuse, 2003), provide an additional but hitherto
49 underutilised tool for determining the basin-scale dynamics of ancient ocean currents (e.g.,
50 Boldreel et al., 1998; Davies et al., 2001; Due et al., 2006; Hohbein et al., 2012). For example,
51 seismic data can image large (up to 10's of metre thick, and several hundred-to-tens of
52 kilometres long), contour current-driven bedforms, which document protracted transport and
53 deposition of biogenic or detrital sediment (e.g. Rebesco and Stow, 2001; Stow et al., 2003),
54 and/or scours of comparable depth, width, and length that record periods of net-seabed erosion
55 and sediment redeposition. If integrated with other, more commonly used paleoceanographic
56 proxies, seismic reflection data could form a key part of the oceanographer's toolkit.

57 In this study we use 2D seismic reflection data from the Ceduna Sub-basin, in the
58 eastern Great Australian Bight to map seismic-scale, Middle Eocene-to-Recent scours and
59 bedforms preserved adjacent to Middle Eocene volcanoes. We suggest these scours and
60 bedforms reflect Middle Eocene initiation of the current now known as the Leeuwin Current.
61 Although its age of initiation is debated, the present Leeuwin Current is the longest (5000 km)
62 and one of the most important ocean currents in the southern hemisphere (see below). By
63 providing physical evidence for ocean current activity, the results of our seismic reflection-
64 based analysis at least broadly support studies proposing a Middle Eocene initiation age for the
65 Leeuwin Current. More generically, our study opens up the exciting possibility that industry
66 seismic reflection data, which are freely available for academic use along this and many other
67 continental margins, if integrated with biostratigraphic and geochemical proxies, can help
68 improve our understanding of deep-time dynamics of the Earth's ancient oceans.

69

70 **Geological Setting.** The Ceduna Sub-basin is located in the Bight Basin, offshore southern
71 Australia (Fig. 1A), and formed in response to Jurassic-to-Early Cretaceous rifting and Early
72 Cretaceous-to-Recent, post-rift thermal subsidence. Numerous submarine volcanoes were
73 emplaced during earliest Middle Eocene magmatism at *ca.* 42 Ma (the ‘Bight Basin Igneous
74 Complex’; Schofield & Totterdell, 2008; Jackson, 2012; Magee et al., 2013), with the
75 volcanoes overlapped by the fully marine, Middle Eocene-to-Recent, carbonate-dominated
76 Nullarbor Limestone (Fig. 1B) (Schofield & Totterdell, 2008). Schofield & Totterdell (2008)
77 and Jackson (2012) identify numerous ‘scours’ in the Nullarbor Limestone, although they do
78 not explore their age or origin, their genetic relationship to the Middle Eocene volcanoes, or
79 the potential paleoceanographic significance of their causal current. There are no direct
80 constraints on Middle Eocene-to-Recent water depths in the distal Ceduna Sub-basin, although
81 Jackson (2012) suggests the basin deepened to a few hundred metres during Middle Eocene
82 flooding (see also McGowran et al., 1997; Shafik, 1983; 1990). The interpreted relatively deep-
83 marine setting is consistent with water depth indicators provided by the heights of Eocene
84 clinoforms preserved along the northern basin margin (Feary and James, 1995, 1998;
85 McGowran et al., 1997). The Ceduna Sub-basin lies outboard of the modern day shelf edge in
86 water depths of 200–4000 m; the seabed in the study area is below the influence of the modern
87 Leeuwin Current, which extends to depths of 300 m (Feng et al., 2009).

88

89 **Paleoceanography of the Great Australian Bight.** The Leeuwin Current is the longest (5000
90 km) coastal current in the world and one of the most important ocean currents in the southern
91 hemisphere (Fig. 1A). It is connected to and thus samples the global thermohaline system via
92 the Indonesian Gateway (Feng et al., 2009), flowing southwards along the western coast of
93 Australia and thereafter eastwards into the Great Australian Bight (Fig. 1A) (Cresswell and
94 Golding, 1980). Transporting warm, low-salinity waters derived from the South Equatorial
95 Current, the Leeuwin Current contributes to climatic variations and vegetation patterns (e.g.,
96 Caputi, 2001; Feng et al., 2009; Wyrwoll et al., 2009), and continent-scale biodiversity patterns
97 by transporting otherwise low-latitude fauna to anomalously high latitudes (e.g., Cann and
98 Clarke, 1993; McGowran et al., 1997; Passlow et al., 1997).

99 The Quaternary extent and dynamics of the Leeuwin Current in the Great Australian
100 Bight are relatively well understood (Cresswell and Golding, 1980; Feng et al., 2009; Wyrwoll
101 et al., 2009), whereas its timing of initiation, and its pre-Quaternary eastward ‘reach’ into the
102 Great Australian Bight, remain uncertain. Based on their discovery of warm-water, Eocene

103 microfauna in the Otway Basin, McGowran et al. (1997) suggested an even older, Middle
104 Eocene age of initiation for the Leeuwin Current in the Great Australian Bight, arguing these
105 fauna were likely derived from warm low-latitudes (i.e. via the proto-Leeuwin Current) and
106 not cold high-latitudes (i.e. via the Flinders Current) (Fig. 1A); this interpretation is supported
107 by fully coupled climate model simulations (Huber et al., 2004). However, pre-Early Oligocene
108 initiation of the Leeuwin Current is disputed given that opening of the Tasmanian Gateway,
109 which facilitated eastwards flow of warm ocean waters along southern Australia into the
110 Pacific, did not occur until the Early Oligocene (e.g. Stickley et al., 2004; Wyrwoll et al., 2009).
111 These studies together suggest the proto-Leeuwin Current in some way shaped the Eocene-to-
112 Recent stratigraphic evolution of the Great Australian Bight shelfal regions, although the
113 stratigraphic expression of time-equivalent, basin-centre units, which should also record the
114 initiation and influence of this important ocean current, has yet to be documented.

115 Although Middle Eocene initiation of the Leeuwin Current is disputed, there is
116 evidence from IODP Leg 182 that anomalously warm waters entered the Great Australian
117 Bight during the middle Miocene, possibly in response changes in ocean circulation driven by
118 the Miocene Climatic Optimum (e.g. Savin et al., 1975; Feary and James, 1995, 1998; Gourley
119 and Gallagher, 2004). For example, McGowran et al. (1997) document the ‘Little Barrier Reef’,
120 a thick (350 m), laterally extensive (>475 km long), rimmed carbonate platform developed
121 along the northern margin of the Bight Basin (Fig. 1A).

122
123 **Data and methods.** Our dataset consists of 109 time-migrated, zero-phase, 2D seismic
124 reflection lines that have a cumulative line length of *c.* 13,000 km and cover *c.* 44,000 km² of
125 the central Ceduna Sub-basin (Fig. 1A). The NW- and NE-trending lines are spaced 4–16 km
126 and 4–8 km, respectively (Fig. 2). The Gnarlyknots-1a borehole constrains the age of four key
127 seismic reflections (Horizons A–D; Figs 1B and 3). This borehole also contains well-log data,
128 indicating the Nullarbor Limestone has a p-wave velocity of 2100 m s⁻¹, thereby allowing us
129 to convert measurements in milliseconds two-way time (ms TWT) to metres (cf. Espurt et al.,
130 2009). Extrusive igneous bodies were identified and mapped using the geometric and
131 geophysical criteria outlined by Totterdell & Schofield (2008), Jackson (2012) and Magee et
132 al. (2013). Intra-Nullarbor scours are characterised by erosional surfaces that truncate and are
133 onlapped by, underlying and overlying reflections respectively (Fig. 3). Although seismic data
134 are only 2D and relatively widely spaced, scours and spatially related ‘hummocky’ seismic
135 facies are typically imaged on and can be mapped between, several adjacent seismic lines. In

136 particular, it is clear that the scours are only developed adjacent to and define ‘moats’ that
137 encircle the volcanic vents (see below and Fig. 2).

138

139 **Description of intra-Nullarbor seismic facies.** We define two main stratal units within the
140 Nullarbor Formation (SU1-2), separated by a major erosional surface (Horizon D; Figs 1 and
141 3). The base of SU1 is defined by a high-amplitude, laterally-continuous, positive seismic
142 reflection defining the contact between the Pidinga Formation and the Nullarbor Limestone
143 (i.e. Horizon B), or a series of volcanoes (i.e. Horizon C) (Figs 1B and 3). SU1 comprises the
144 lower part of the Nullarbor Limestone and, away from the volcanoes, is typically characterised
145 by low-to-moderate amplitude, parallel-to-sub-parallel, very continuous reflections (Fig. 3).
146 Closer to the volcanoes (i.e. <2 km), a series of gently-dipping (<4°) reflections are developed
147 in SU1, and these locally display bilateral downlap onto the underlying reflections and thus
148 define convex-up, ‘mounded’ bodies (Figs 3B-D). These inclined reflections, which either dip
149 towards (Fig. 3A) or away (Figs 3C–D) from the volcanoes, typically overlie low-angle (<6°)
150 erosional surfaces, which are up to 2 km wide and display up to 100 m of relief; these surfaces
151 pass laterally into (seismically) conformable surfaces (Fig. 3).

152 The base of SU2 is locally defined by a major erosion surface along which numerous
153 scours are developed (Horizon D; Figs 1–3). These scours locally define a series of ‘moat-like’
154 features that fully or partly encircle 15 of the 57 vents present in the Ceduna Sub-basin (e.g.
155 Fig. 2). The scours have a relief of 10–90 m, extend <3 km from the volcanoes, and their flanks
156 dip 0.1–6.1°, being best-developed around volcanoes that are typically >200 m tall. Some of
157 the scours are asymmetric, consisting of a long, gently dipping outer margin inclined towards
158 the vents and a shorter, more steeply-dipping surface that dips away from the vents (Figs 3B–
159 D). Our 2D seismic data do not allow us to confidently determine if the scours are preferentially
160 developed on one side of the vents (Fig. 2). Two main types of seismic facies fill the scours:
161 (i) high-amplitude, ‘hummocky’ reflections, which have a relief of up to 50 m and a distance
162 of 100–200 m between adjacent hummock crests (Fig. 3B); and (ii) low-to-high amplitude,
163 gently-dipping (<2°), moderately discontinuous to laterally-continuous reflections (Fig. 3). The
164 upper part of SU2 is dominated by low-to-high amplitude, flat-lying to gently-dipping (<2°),
165 laterally-continuous reflections (Fig. 3), with erosionally based packages of chaotic reflections
166 locally being developed.

167

168 **Interpretation of intra-Nullarbor features.** Based on their development in a fully marine
169 succession and given that post-Middle Eocene water depths were probably at least several

170 hundred metres (see Jackson, 2012), it is unlikely the intra-Nullarbor scours and hummocks
171 formed subaerially. Furthermore, the coeval basin margin, which was likely located several
172 hundred kilometres to the north, was carbonate-dominated and constructional (Fig. 1; see also
173 Feary and James, 1995, 1998), suggesting little or no sediment bypass was occurring, and that
174 voluminous, strongly erosional, deep-water gravity currents, such as turbidity currents, did not
175 form the intra-Nullarbor scours and hummocks.

176 Based on their development in a fully marine succession deposited in several hundreds
177 of metres of water, our preferred interpretation is that the scours formed in response to ocean
178 current-related incision of the seabed (Fig. 4). Such scours are common in modern seas and
179 oceans, typically in association with channel-related contourite drifts (*sensu* Stow et al., 2002).
180 The spatial restriction of Ceduna Sub-basin scours to within c. 3 km of the volcanoes, strongly
181 suggests the volcanic edifices formed syn-incision bathymetric highs that perturbed the
182 velocity structure of the causal ocean currents. We suggest this perturbation increased current
183 turbulence and, most critically, seabed shear stress, driving localised erosion of the seabed
184 immediately adjacent to the volcanoes (Fig. 4) (e.g. O'Reilly et al., 2003; MacLachlan et al.,
185 2008). Submarine scours of broadly similar geometry, dimension, and origin are observed
186 adjacent to igneous rock-cored bathymetric highs in the Pisces Reef system, Irish Sea, UK
187 (Callaway et al., 2009), and in the Capel and Faust basins, offshore eastern Australia (Rollet et
188 al., 2012).

189 We interpret that inclined and hummocky reflections developed throughout the
190 Nullarbor Limestone represent dip-oblique and dip-parallel sections, respectively, through
191 sediment wave- or contourite drift-like deposits (cf. Rebesco and Stow, 2001; Stow et al., 2003;
192 Hohbein et al., 2012). Sedimentary bodies like this are commonly associated with seabed
193 scours, being deposited when bottom current energy is low enough to permit sediment
194 reworking within bedforms (Fig. 4) (e.g. Stow et al., 2002). Like the scours, intra-Nullarbor
195 bedforms are spatially restricted to within a few kilometres of the vents, suggesting they too
196 formed due to volcano-driven perturbations in ocean current velocity and seabed shear stress.
197 In their case, however, an increase in seabed shear stress was only sufficient to rework sediment
198 and not deeply erode the seabed (Fig. 4).

199

200 **Implications for the paleoceanographic development of the Great Australian Bight.**

201 Although the Gnarlyknots-1a borehole penetrates the Nullarbor Formation, no biostratigraphic
202 data were collected; as a result, we cannot constrain the age of intra-Nullarbor scours,
203 associated strata, or indeed, the causal current more tightly than 'Middle Eocene-to-Recent'.

204 Furthermore, no paleobathymetric data (e.g. benthic foraminifera) were collected in
205 Gnarlyknots-1a, meaning we have no direct constraints on water depth variations during the
206 Middle Eocene-to-Recent, and thus the depth of formation of the ocean current-related scours
207 and bedforms remains uncertain (see also discussion in Jackson, 2012). Our relatively widely
208 spaced 2D seismic reflection data also do not allow us to confidently determine if intra-
209 Nullarbor scours are preferentially developed on one, most likely the down-current (i.e. lee)
210 side of the seabed obstruction (i.e. the volcanoes), or if the associated bedforms are best-
211 developed on one, most likely the up-current side of the vents, and display down-current
212 accretion (e.g. Callaway et al., 2009; Rollet et al., 2012). Because of this, we do not know the
213 dominant direction of the causal current.

214 Notwithstanding these limitations, it is informative to discuss the implications of our
215 study for the Paleogene paleoceanographic evolution of the eastern Great Australian Bight.
216 Using biostratigraphic proxy data from the Bight and Otway basins, McGowran et al. (1997)
217 suggest the initiation of eastwards protrusion of a so-called ‘proto-Leeuwin Current’ into the
218 Great Australian Bight during the Middle Eocene, with further evidence for its presence in the
219 middle Miocene (Fig. 1A; see also Feary and James, 1995, 1998). This interpretation was,
220 however, challenged by Wyroll et al. (2009), who suggest these fauna may simply record
221 locally elevated sea surface temperatures unrelated to the initiation of a plate-scale
222 thermohaline current. We here suggest Middle Eocene-to-Recent scours and bedforms
223 developed in the Ceduna Sub-basin are associated with Paleogene initiation of an
224 oceanographic current, which we link to the postulated proto-Leeuwin Current (Fig. 4). More
225 specifically, we propose these features record late Middle Eocene initiation and subsequent
226 fluctuations in the strength and erosivity of, the current. The major intra-Nullarbor erosion
227 surface (Horizon D), for example, which is best-developed immediately adjacent to the
228 volcanoes, may represent intensification or ‘waxing’ of the proto-Leeuwin Current (Fig. 4).
229 Despite a lack of age data, we tentatively suggest this erosional event, and related bedforms,
230 may be the stratigraphic expression of the Miocene Climatic Optimum-related event proposed
231 by Feary and James (1995, 1998), during which time anomalously warm waters encroached
232 eastwards into the Great Australian Bight from western Australian (see also Savin et al., 1975;
233 Gourley and Gallagher, 2004).

234 Our study shows that seismic reflection data can image erosional and depositional
235 features that provide a physical stratigraphic record of ancient ocean currents. We demonstrate
236 that by placing these features into a broad chronostratigraphic framework, we can complement
237 rather sparse micro-faunal evidence, and gain important insights into the timing of onset of

238 major ocean currents. Data limitations notwithstanding, our seismic reflection-based approach
239 does, at the very least, provide a clear hypothesis testable with future scientific drilling (e.g.
240 IODP). Seismic reflection data allow erection of a physical, stratigraphic framework and may
241 be an essential part of the paleoceanographer's toolkit. Future work should focus on detailed
242 mapping of seismic reflection datasets from, for example, the western Bight Basin and Otway
243 Basin; this may reveal similar, age-equivalent current-formed stratigraphic features, thus
244 raising the possibility that the proto-Leeuwin Current extended further eastwards and
245 influenced faunal distribution and potentially climate over a wider area than currently assumed.

246

247 **ACKNOWLEDGEMENTS**

248 Geoscience Australia are thanked for providing seismic and borehole data.

249

250 **REFERENCES**

251

252 Boldreel, L.O.L., Andersen, M.S., and Kuijpers, A., 1998, Neogene seismic facies and deep-
253 water gateways in the Faeroe Bank area, NE Atlantic: *Marine Geology*, v. 152, p. 129-140.

254

255 Callaway, A., Smyth, J., Brown, C.J., Quinn, R., Service, M., and Long, D., 2009, The impact
256 of scour processes on a smothered reef system in the Irish Sea: *Estuarine, Coastal and Shelf
257 Science*, v. 84, p. 409–418.

258

259 Caputi, N., Chubb, C.F., and Pearce, A., 2001, Environmental effects on recruitment of the
260 western rock lobster, *Panulirus Cygnus*: *Marine and Freshwater Research*, v. 52, p. 1167-1175.

261

262 Cann, J.H., and Clarke, J.A.D., 1993, The significance of *Marginopora vertebralis*
263 Foraminifera in surficial sediments at Esperance, Western Australia and in last interglacial
264 sediments in northern Spencer Gulf: *Marine Geology*, v. 111, p. 171–187.

265

266 Cartwright, J.A., and Huuse, M., 2005, 3D seismic technology: the geological 'Hubble'. *Basin
267 Research*, 17, p. 1-20.

268

269 Cresswell, G., and Goldring, T., 1980, Observations of a south-flowing current in the
270 southeastern Indian Ocean: *Deep Sea Research Part 1: Oceanographic Research Papers*, v. 27,
271 p. 449-466.

272
273 Davies, R.J., Cartwright, J.A., Pike, J., and Line, C., 2001, Early Oligocene initiation of North
274 Atlantic deep water formation: *Nature*, v. 410, p. 917-920.
275
276 Due, L., van Aken, H.M., Boldreel, L.O., and Kuijpers, A., 2006, Seismic and oceanographic
277 evidence of present-day bottom-water dynamics in the Lousy Bank-Hatton Bank area, NE
278 Atlantic. *Deep Sea Research Part 1: Oceanographic Research Papers*, v. 53, p. 1729-1741.
279
280 Espurt, N., Callot, J-P., Totterdell, J., Struckmeyer, H., and Vially, R., 2009, Interaction
281 between continental breakup dynamics and large-scale delta system evolution: insights from
282 the Cretaceous Ceduna delta system, Bight Basin, southern Australian margin: *Tectonics*, v.
283 28, TC6002.
284
285 Feary, D.A., and James, N.P., 1995, Cenozoic biogenic mounds and buried Miocene (?) barrier
286 reef on a predominantly cool-water carbonate continental margin, Eucla Basin, western Great
287 Australian Bight: *Geology*, v. 23, p. 427-430.
288
289 Feary, D.A., and James, N.P., 1998, Seismic Stratigraphy and Geological Evolution of the
290 Cenozoic, Cool-Water Eucla Platform, Great Australian Bight: *AAPG Bulletin*, v. 82, p. 792-
291 816.
292
293 Feng, M., Waite, A., and Thompson, P., 2009, Climate variability and ocean production in the
294 Leeuwin Current system off the west coast of Western Australia: *Journal of the Royal Society
295 of Western Australia*, v. 92, p. 67-81.
296
297 Gourley, T.L., and Gallagher, S.J., 2004, Foraminiferal biofacies of the Miocene warm to cool
298 climatic transition in the Port Phillip Basin, southeastern Australia: *Journal of Foraminiferal
299 Research*, v. 34, p. 294-307.
300
301 Henderson, G.M., 2002, New oceanic proxies for paleoclimate, *Earth and Planetary Science
302 Letters*, v. 203, 1-13.
303

304 Hohbein, M., Sexton, P.F., and Cartwright, J.A., 2012, Onset of North Atlantic Deep Water
305 production coincident with inception of the Cenozoic global cooling trend: *Geology*, v. 40, p.
306 255-258.

307

308 Huber, M., Brinkhuis, H., Stickley, C.E., Döös, K., Sluijs, A., Warnaar, J., Schellenberg, S.A.,
309 and Williams, G.L., 2004, Eocene circulation of the Southern Ocean: Was Antarctica kept
310 warm by subtropical waters? *Paleoceanography*, v. 19, PA4026.

311

312 IPCC, 2007, *Climate Change 2007: The physical science basis. Contribution of Working*
313 *Group I to the Fourth Assessment Report of the Intergovernmental Panel on Climate Change*
314 (eds. Solomon, S., Qin, D., Manning, M., Chen, Z., Marquis, M., Averyt, K.B., Tignor, M.,
315 and Miller, H.L). Cambridge University Press, Cambridge.

316

317 Jackson, C.A-L., 2012, Seismic reflection imaging and controls on the preservation of ancient
318 sill-fed magmatic vents: *Journal of the Geological Society*, v. 169, p. 503-506.

319

320 MacLachlan, S.E., Elliott, G.M., and Parsons, L.M., 2008, Investigations of the bottom current
321 sculpted margin of the Hatton Bank, NE Atlantic: *Marine Geology*, v. 253, p. 170-184.

322

323 Magee, C., Hunt-Stewart, E., and Jackson, C.A-L., 2013, Volcano growth mechanisms and the
324 role of sub-volcanic intrusions: Insights from 2D seismic reflection data: *Earth and Planetary*
325 *Science Letters*, 373, p. 41-53.

326

327 McGowran, B., Qianyu, L., Cann, J., Padley, D., McKirdy, D.M., and Shafik, S., 1997,
328 Biogeographic impact of the Leeuwin Current in southern Australia since the late Middle
329 Eocene: *Palaeogeography, Palaeoclimatology, Palaeoecology*, v. 136, p. 19-40.

330

331 O'Reilly, B., Readman, P.W., Shannon, P.M., and Jacob, A.W.B., 2003, A model for the
332 development of a carbonate mound population in the Rockall Trough based on deep-towed
333 sidescan sonar data: *Marine Geology*, v. 198, p. 55-66.

334

335 Rahmstorf, S., 2003, The current climate: *Nature*, v. 421, p. 699.

336

337 Rebesco, M., and Stow, D., 2001, Seismic expression of contourites and related deposits: a
338 preface: *Marine Geophysical Researches*, v. 22, p. 303–308.
339

340 Rollet, N., McGiveron, S., Hashimoto, T., Hackney, R., Petkovic, P., Higgins, K., Grosjean,
341 E., Logan, G.A., 2012, Seafloor features and fluid migration in the Capel and Faust basins,
342 offshore eastern Australia: *Marine and Petroleum Geology*, v. 35, p. 269–291.
343

344 Savin, S.M., Douglas, R.G., and Stehli, F.G., 1975, Tertiary marine paleotemperatures:
345 *Geological Society of American Bulletin*, v. 86, p. 1499–1510.
346

347 Schofield, A., and Totterdell, J., 2008, Distribution, timing and origin of magmatism in the
348 Bight and Eucla basins: Australian Government Report, 2008/24.
349

350 Shafik, S., 1983, Calcareous nannofossil biostratigraphy: an assessment of foraminiferal and
351 sedimentation events in the Eocene of the Otway Basin, southeastern Australia: *Journal of*
352 *Australian Geology and Geophysics*, v. 8, p. 1-17.
353

354 Shafik, S., 1990, The Maastrichtian and early Tertiary record of the Great Australian Bight
355 Basin and its onshore equivalents on the Australian southern margin: a nannofossil study:
356 Bureau of Mineral Resources *Journal of Australian Geology and Geophysics*, v. 11, p. 473-
357 497.
358

359 Stickley, C.E., Brinhuis, H., Schellenberg, S.A., Sluijs, A., Röhl, U., Fuller, M., Grauert, M.,
360 Huber, M., Warnaar, J., and Williams, G.L., 2004, Timing and deepening of the Tasmanian
361 Gateway. *Paleoceanography*, v. 19: PA4027.
362

363 Stow, D.A.V., Faugères, J.C., Howe, J.A., Pudsey, C.J., and Viana, A.R., 2003, Bottom
364 currents, contourites and deep-sea sediment drifts: Current state-of-the-art, in Stow, D.A.V., et
365 al., eds., *Deep-water contourite systems: Modern drifts and ancient series, seismic and*
366 *sedimentary characteristics: The Geological Society of London Memoir*, v. 22, p. 73–84.
367

368 von Blanckenburg, F., 1999, Palaeoceanography: tracing past ocean circulation?: *Science*, v.
369 286, p. 1862-1863.
370

371 Wunsch, C., 2002, What is the thermohaline circulation?: Nature, v. 298, p. 1179-1181.

372

373 Wyrwoll, K-H., Greenstein, B.J., Kendrick, G.W., and Chen, G.S., 2009, The
374 palaeoceanography of the Leeuwin Current: implications for a future world. Journal of the
375 Royal Society of Western Australia, v. 92, p. 37–51.

376

377 **FIGURE CAPTIONS**

378

379 **Fig 1.** (A) Map illustrating the geographical setting of the study area. The area covered by 2D
380 seismic reflection data is outlined by a solid black line. Inset shows the key modern
381 oceanographic currents developed along the western and southern Australian margin.
382 LC=Leeuwin Current; ACC=Antarctic Circumpolar Current; WAC=West Australia Current;
383 FC=Flinders Current. OB=Otway Basin. Modified from Jackson (2012); oceanographic
384 currents from Bilj et al. (2013). (B) Simplified stratigraphic column based on data from
385 boreholes Gnarlyknots-1A and Potoroo-1. Key seismic horizons (A–D) and seismic units
386 (SU1-2) are indicated. The stratigraphic occurrence of intrusion and extrusive components of
387 the Bight Basin Igneous Complex (BBIC) are shown. Modified from Jackson (2012).

388

389 **Fig. 2.** Time-structure map of the Horizon D merged with a time-structure map of Horizon C;
390 this illustrates the distribution of volcano summits (labelled ‘v’ and encircled by a solid white
391 line) that rise above Horizon D, and intra-SU2 moats (labelled ‘m’). sw=sediment wave crests.
392 (A) and (B) are from the southern and northern parts of the study area respectively. See Figure
393 1A for location of map. Light grey lines indicate seismic reflection profiles.

394

395 **Fig. 3.** (A)–(D) Interpreted seismic profiles illustrating the geometry, scale and relationship
396 between extrusive volcanic features of the Bight Basin Igneous Complexes and intra-Nullarbor
397 Limestone scours (moats) and bedforms. Locations of the seismic lines are shown in Figure 2.
398 Uninterpreted versions of sections are available in DRI1.

399

400 **Fig. 4.** (A–C) Schematic diagrams illustrating the evolution of intra-Nullarbor Limestone
401 scours in the Great Australia Bight. The vertical dashed line in the ‘current strength’ column
402 indicates the threshold for sediment erosion/non-deposition; these conditions occur at the onset
403 of T2.

404

405 **Data Repository Item (DR1).** Uninterpreted versions of the seismic profiles presented in Fig.
406 3.

Fig. 1

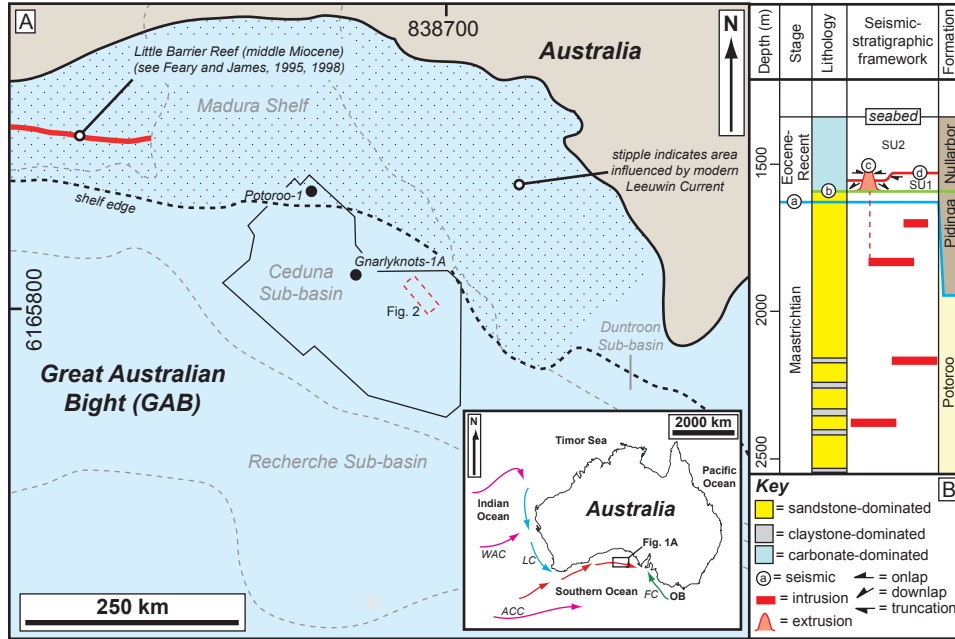


Fig. 2

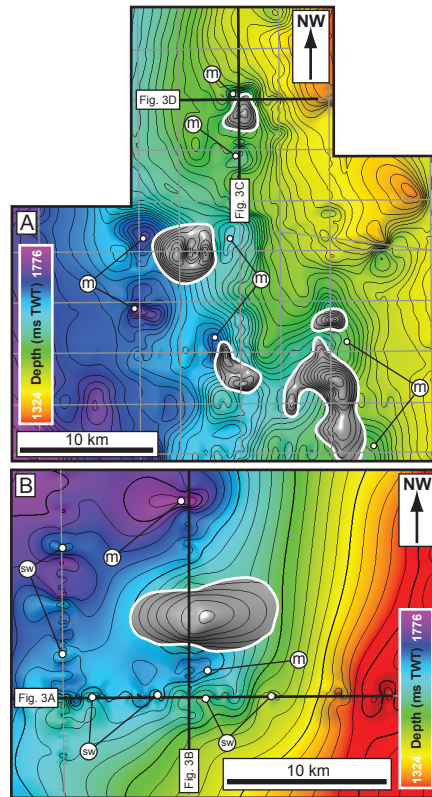


Fig. 3

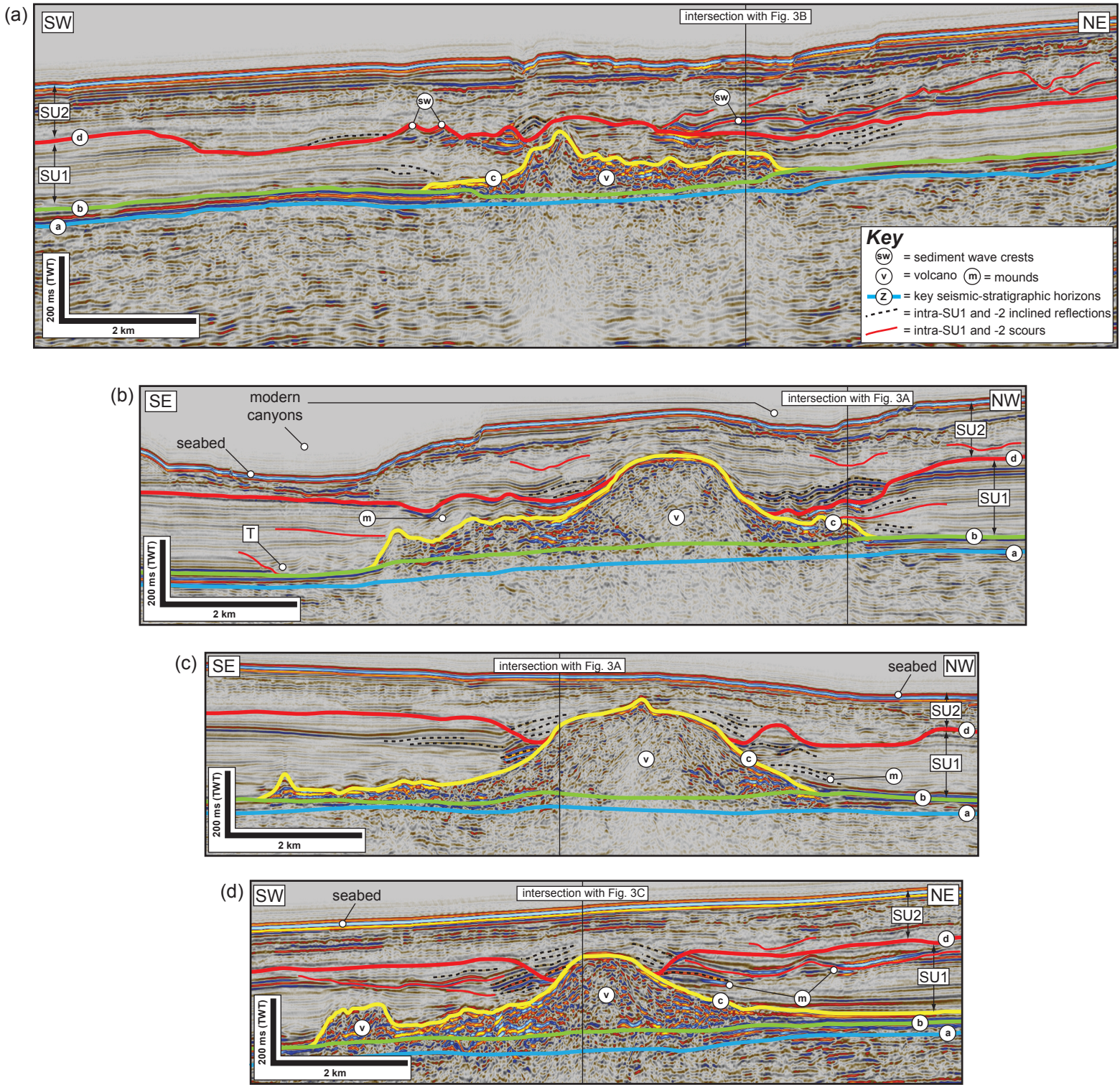
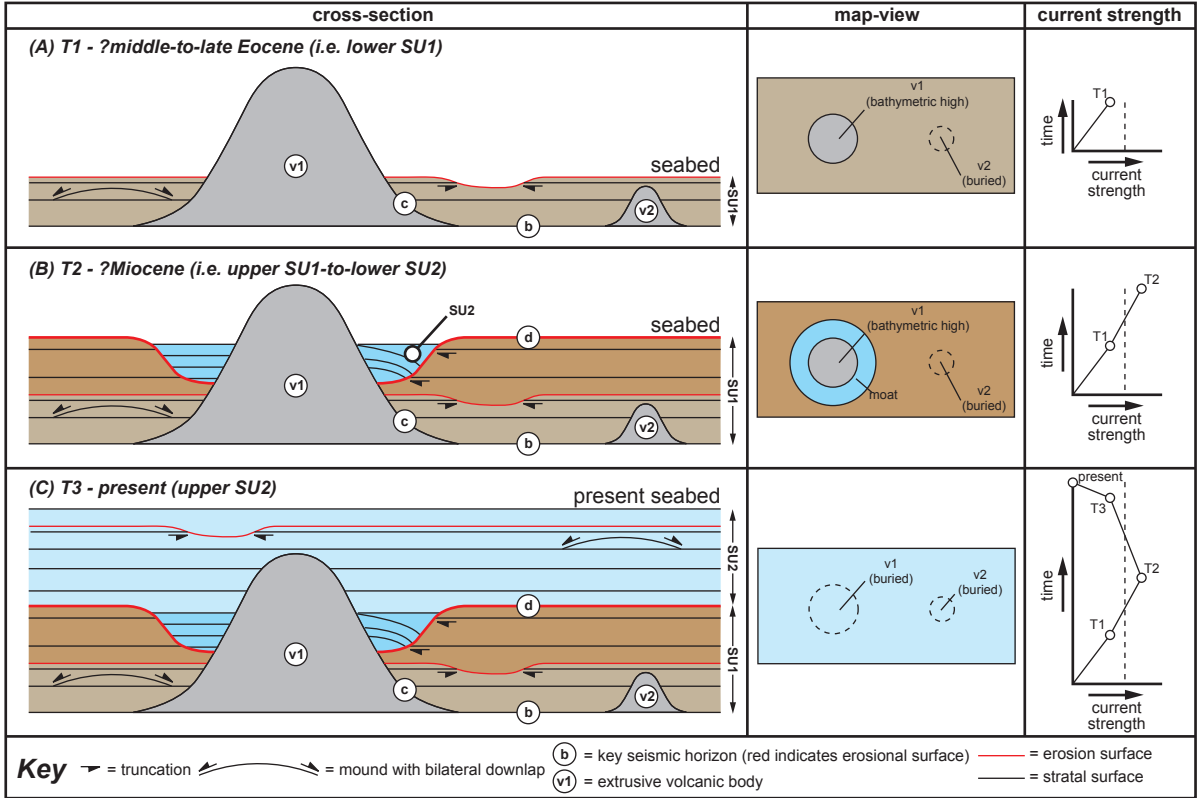


Fig. 4



Data Repository Item 1 (DR1)

